Josephson parametric converter saturation and higher order effects

G. Liu, T.-C. Chien, X. Cao, O. Lanes, E. Alpern, D. Pekker, and M. Hatridge[a)]
Department of Physics and Astronomy, University of Pittsburgh, Pittsburgh, Pennsylvania 15260, USA

(Received 1 September 2017; accepted 29 October 2017; published online 14 November 2017)

Microwave parametric amplifiers based on Josephson junctions have become indispensable components of many quantum information experiments. One key limitation which has not been well predicted by theory is the gain saturation behavior which limits the amplifier's ability to process large amplitude signals. The typical explanation for this behavior in phase-preserving amplifiers based on three-wave mixing, such as the Josephson Parametric Converter, is pump depletion, in which the consumption of pump photons to produce amplification results in a reduction in gain. However, in this work, we present experimental data and theoretical calculations showing that the fourth-order Kerr nonlinearities inherent in Josephson junctions are the dominant factor. The Kerr-based theory has the unusual property of causing saturation to both lower and higher gains, depending on bias conditions. This work presents an efficient methodology for optimizing device performance in the presence of Kerr nonlinearities while retaining device tunability and points to the necessity of controlling higher-order Hamiltonian terms to make further improvements in parametric devices. *Published by AIP Publishing*. https://doi.org/10.1063/1.5003032

Quantum-limited amplifiers are a vital tool in quantum information processing. At microwave frequency, such amplifiers enable high-fidelity measurements of quantum bits,[1,2] nano-mechanical resonators,[3] and flying states of light.[4] The amplifiers are typically built from microwave resonators containing one or more superconducting Josephson junctions, which provide the essential non-linear Hamiltonian terms and hence their collective description as Josephson Parametric Amplifiers (JPAs).[5–12] The strength of the non-linear coupling between the device's modes is controlled via an external microwave pump, which in turn sets the amplifiers' gain and center frequency.

A JPA's utility is determined by several parameters. These include its quantum efficiency, which describes the noise added during amplification,[13] tunability to match the signal frequency of interest, instantaneous bandwidth,[14,15] and the ability to process large amplitude signals. The last parameter is typically referred to as the saturation power or more precisely as $P_{-1\mathrm{dB}}$, the input power at which the gain falls by 1 dB from its small signal value. Conventionally, saturation in JPAs is attributed to depletion of photons from the microwave pump tone.[16–18] The pump both controls the amplifier gain and serves as the power source for photons created in the amplification process, resulting in a monotonic decrease in gain with increasing signal power.

However, pump depletion has, in almost all cases, failed to give an accurate description of experimental device performance.[16,17] In this letter, we show that, instead, Kerr nonlinearities inherent to Josephson junctions are the dominant factor that limits device saturation power. Our results give good qualitative agreement between a theory which completely neglects pump depletion and experimental data for phase preserving amplification in the Josephson Parametric Converter (JPC).[19,20] We find that for typical device parameters, the Kerr terms of the Hamiltonian cause the system to dispersively shift away from its bias point before the effects of pump-depletion become relevant.

Given this understanding, we present a methodology for optimizing device performance in the presence of Kerr nonlinearities while retaining device tunability. Although in this paper we specifically study amplifiers based on three-wave mixing with the Josephson Ring Modulator (JRM),[16] this effect will be equally prominent in three-wave mixing devices based on SQUIDS or other multi-junction circuits with similar-amplitude Kerr terms.[21] We note that a related effect has been studied theoretically for the case of single junction four-wave mixing based amplifiers.[22]

The JPC realizes non-degenerate three-wave mixing with a ring of four nominally identical Josephson junctions (the JRM), placed at the intersection of two $\lambda/2$ resonators (see Fig. 1). The horizontal mode is referred to as the idler or a-mode, while the vertical mode is the signal or b-mode. There is a third, common mode, c, consisting of a joint excitation of the horizontal and vertical spatial modes. The idler and signal mode are each strongly coupled to a single microwave port accessible through transmission lines with decay rates $\kappa_{a,b}$, while the pump tone is coupled to the c mode via a weakly coupled pump port. The device tunability is enhanced by the addition of four interior junctions, which are much larger than the outer junctions that produce the three-wave mixing and as such are treated as linear inductors.[23] Up to third order in creation/annihilation operators, the Hamiltonian of the JPC in the rotating wave approximation can be written as[19]

$$\frac{H_{\mathrm{JPC}}}{\hbar} = \omega_a a^\dagger a + \omega_b b^\dagger b + \omega_c c^\dagger c + g(a^\dagger b^\dagger c + abc^\dagger), \quad (1)$$

where a, b, and c are the annihilation operators of the three modes of the JPC, and g is the flux-dependent three-wave coupling strength. Gain is achieved by applying a strong microwave drive to spatial mode c at the frequency $\omega_p \simeq \omega_a + \omega_b$. If this is strongly detuned from any c-mode resonance,

a)hatridge@pitt.edu.

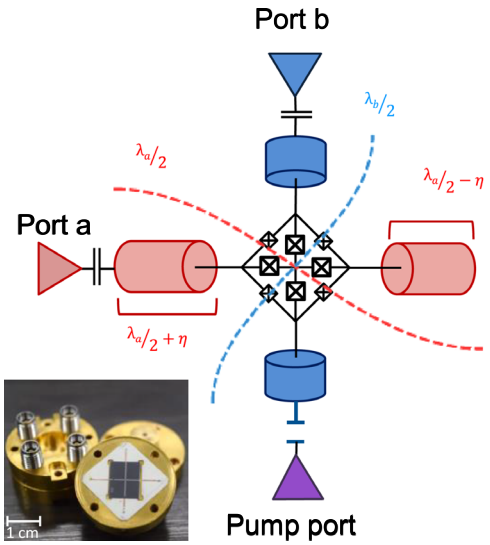

FIG. 1. Schematic of a single-ended Josephson Parametric Converter (JPC) circuit. The device consists of two $\lambda/2$ resonators which meet at a central ring of Josephson junctions, the JRM. The horizontal (red) mode is labeled a, the vertical (blue) mode b, and there is a third, common mode c of the two arms. Resonant modes a and b are each strongly coupled to a single microwave port, and the pump is weakly coupled via the pump port. (Inset) Image of assembled JPC. The a and b modes and pump port are each accessed through individual SMA connectors.

the pump is said to be "stiff," meaning that c can be replaced with its average value. In this letter, we calculate the average response of the amplifier using semi-classical Langevin equations derived from the circuit Hamiltonian, together with the modes' coupling rates to the microwave environment (see supplementary material, Sec. I).

The flux dependence of the mode frequencies $\omega_{a,b}$ allows amplification over a wide range of frequencies by varying the flux applied to the JRM. At a fixed flux, the amplifier can be further tuned over a narrower range of frequencies, roughly corresponding to mode bandwidths $\kappa_{a,b}$, by varying the pump frequency away from the sum frequency by ϵ, so that $\omega_p = \omega_a + \omega_b + \epsilon$. Note that for each pump frequency, there is a unique peak gain frequency which depends on both the pump detuning and the mode bandwidths. For $\kappa_{a,b} = \kappa \mp \Delta\kappa/2$, the peak gain frequency (for mode a) can be written to first order in ϵ and $\Delta\kappa$ as $\omega_{\mathrm{maxG}} = \omega_a + \left(\frac{1}{2} - \frac{\kappa\Delta\kappa/2}{4g^2\langle c\rangle^2+\kappa^2+(\Delta\kappa/2)^2}\right)\epsilon$ (see supplementary material, Sec. I).

In the JPC Hamiltonian, the 4th order (Kerr) nonlinearity, which is typically neglected in Eq. (1), is

$$\frac{H_{\mathrm{Kerr}}}{\hbar} = -\sum_{m=a}^{c}\sum_{n=m}^{c} K_{mn} a_m^\dagger a_m a_n^\dagger a_n, \tag{2}$$

where $a_i = (a, b, \text{and } c)$ and K_{mn} are the Kerr amplitudes (see supplementary material, Sec. II). Given the stiffness of the pumped c mode, the K_{cc} term is a constant for a given set of pump conditions and can be neglected, leaving five terms to be considered. Of these, the K_{ac} and K_{bc} are simplified by the stiff pump approximation to be pump-dependent Stark shifts of the a and b modes. Their effect is visible even at very low signal power as they shift the optimal pump frequency (defined as the frequency requiring minimum pump power for achieving a given gain for very low signal powers) to be smaller than the sum frequency of the a and b modes.

The final three terms, K_{aa}, K_{bb}, and K_{ab}, grow with signal power and give a further nonlinear contribution to the amplifier response. Their contributions are largely indistinguishable, as the process of phase-preserving amplification results in very tightly correlated a and b mode populations.[24] The increasing signal amplitude causes the coupled modes to shift to lower resonant frequencies and increased nonlinear response as a function of signal power, reminiscent of the behavior of single mode Duffing oscillators.[25,26] In general, we can only solve these equations numerically: to gain an intuitive picture of the system's behavior as a function of signal power, we calculate the pump power which gives fixed power gain G at different pump frequencies for varying signal powers (see supplementary material, Sec. II). The results are shown in Fig. 2(a) where there is an apparent shift of the curve to lower frequencies and higher pump powers as the coupled modes dispersively shift away from the pump tone.

All experimental data were taken from a single-ended JPC shown schematically in Fig. 1. The need for hybrids to couple symmetrically to the a and b modes has been eliminated. The resulting asymmetry between the two ends of the resonators shifts the current anti-nodes away from the JRM

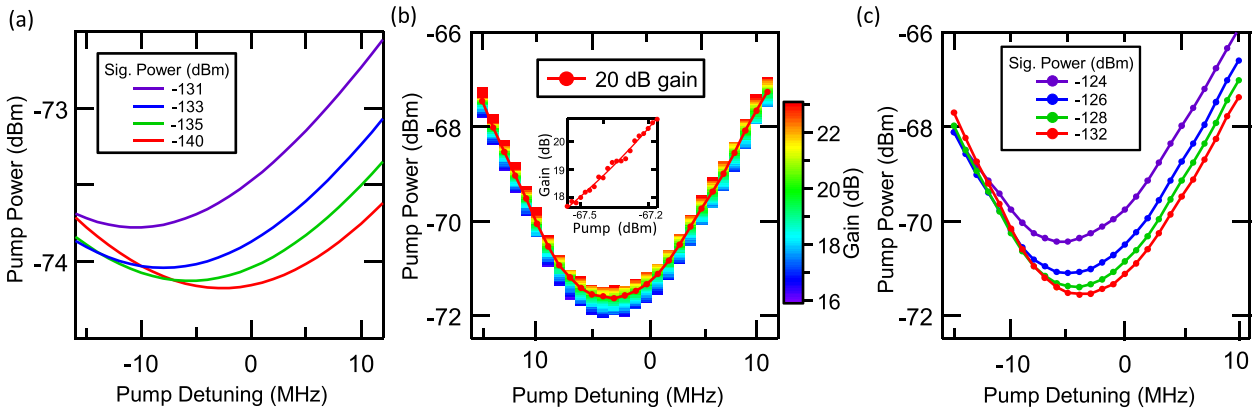

FIG. 2. (a) 20 dB gain curve for different signal powers. (b) Maximum gain vs. pump detuning $[\omega_p - (\omega_a + \omega_b)]$ and power for -150 dBm signal power. Each pixel represents the fitted maximum gain for a pump power/detuning combination. The red line connects all the 20 dB points obtained from fitting gain data at each pump detuning vs pump power (see inset for example fit curve). (c) Experimental $G = 20$ dB points versus pump detuning and power for varying signal powers.

and results in leakage between modes a and b. We correct this effect by introducing an offsetting asymmetry (η) in the length of the two arms of each resonator as indicated in the figure. The device is fabricated using double-angle aluminum deposition of Josephson junctions and resonator on silicon together with a 1.5 μm silver ground plane on the reverse side. The critical current for the outer junctions is 1.78 μA and for the inner junctions is 5.34 μA. The modes a, b, and c are each accessed through individual SMA connectors (see Fig. 1 inset).

For all data, an external DC magnetic flux, $\Phi_{ext} = 1.2\ \Phi_0$, was applied, where $\Phi_0 = h/2e$ is the magnetic flux quantum and we define the flux as applied to the full JRM (which with its four loops is periodic with $4\Phi_0$ total applied flux). At this flux, the resonant frequencies of modes a and b are $\omega_a/2\pi = 5.083$ GHz and $\omega_b/2\pi = 7.452$ GHz, and the linewidths are $\kappa_a/2\pi = 20$ MHz and $\kappa_b/2\pi = 56$ MHz. We first identified the combination of pump powers and frequencies yielding $G = 20$ dB, as shown in Fig. 2(b). For each pixel, a pump power and frequency combination was applied to the pump port, and the small-signal response for $P_{sig} = -150$ dBm was recorded. Each curve was first fitted to identify the maximum gain and associated signal frequency. We found that the most accurate bias conditions were identified by subsequently fitting all peak-gain points at a given pump frequency to the expect response of G vs. P_p, as shown in the inset. Compared to Fig. 2(a), the pump power needed for 20 dB gain increases more rapidly with pump detuning in the data, which is due to impedance variation of the external 50 Ω environment to which the JPC couples.[15]

Next, we evaluated the influence of increasing signal power by repeating this protocol for increasing signal powers, as shown in Fig. 2(c). As the signal power increases, the amplifier response shifts to lower frequency in excellent qualitative agreement with the calculated results shown in Fig. 2(a), including the asymmetry between positive and negative detunings. For positive detunings, the modes shift away from the bias point, and thus, higher pump power is required to maintain 20 dB gain. For negative detunings, the situation is at first reversed as the modes move closer, resulting in an initial shift to *higher* gain before they, too, fall as the modes continue to shift with increasing signal power.

This anomalous behavior requires us to modify how we evaluate saturation; otherwise, we may assign very high saturation powers to an amplifier whose response is extremely nonlinear. A more symmetric limit of $P_{\pm 1\mathrm{dB}}$, defined as the power at which the gain first deviates in either direction by 1 dB from its small signal value, will give a much fairer comparison of different bias conditions.

The amplifier's saturation behavior was measured as shown in Fig. 3. For each pump frequency, we recorded gain vs. signal power while using the pump power and signal frequency determined in Fig. 2(b). The full dataset is shown in Fig. 3(b); for clarity, representative curves are plotted separately in Fig. 3(a). The calculated saturation curves using extracted device parameters (see supplementary material, Sec. II) are plotted in Fig. 3(c). For both data and calculation, the gain initially increases with signal power at negative detuning before finally falling, and for positive detunings, the gain monotonically decreases. The ±1 dB saturation values are indicated by blue diamonds and red triangles, respectively.

At positive detunings, the $P_{-1\mathrm{dB}}$ limit is reached first, in both theory and experiment, eventually leveling off at a value 5–10 dB lower [Fig. 3(a) blue and purple data] than the optimal monotonically decreasing gain point [Fig. 3(a) in green], which is found very near the small-signal resonant condition. For negative detunings, the gain rise phenomenon becomes increasingly severe [Fig. 3(a) in red], eventually resulting in unstable/hysteretic gain conditions (not shown). However, for modestly negative detuning, the gain rise phenomenon can act to enhance the saturation power. Thus, we identify an alternate optimum bias condition [Fig. 3(a) in orange] which rises to just less than +1 dB before falling. Taken together, these factors can result in amplifier performance that varies by well over 10 dB if the amplifier is biased without knowledge of the Kerr effect. As most amplifiers operate over a modest range of bandwidths (10s–100s of MHz) and critical currents (few μA), these behaviors should be visible in all devices and are, in fact, visible in

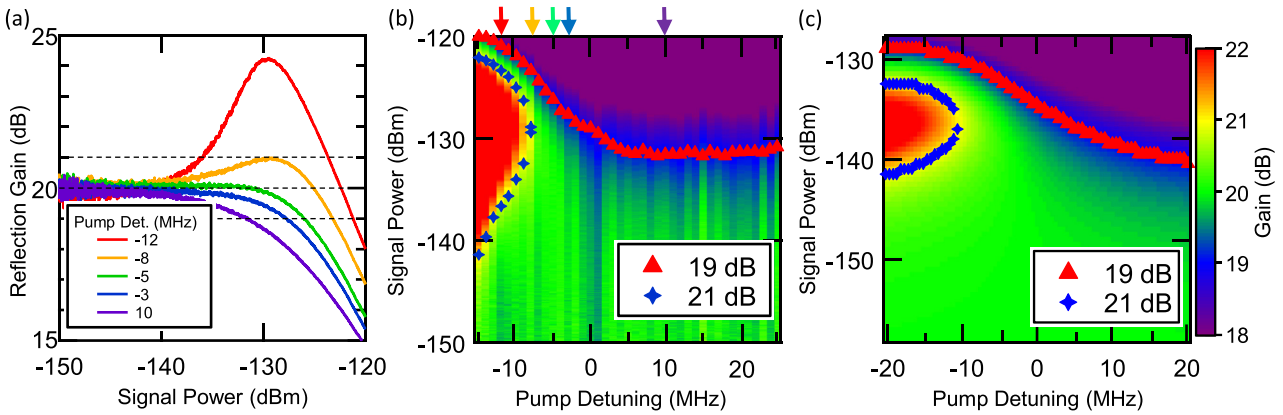

FIG. 3. (a) Measured reflection gain of the JPC vs. signal power at selected pump detunings, showing the variation in saturation response vs pump detuning from the resonant condition. (b) Measured gain vs. signal power and pump detuning for 20 dB bias conditions identified in Fig. 2(b). The colored arrows indicate the dynamic range curves in (a). (c) Calculated theoretical gain at different signal powers and pump detunings. In both (b) and (c), the saturation values are indicated as red triangles (–1 dB) and blue diamonds (+1 dB).

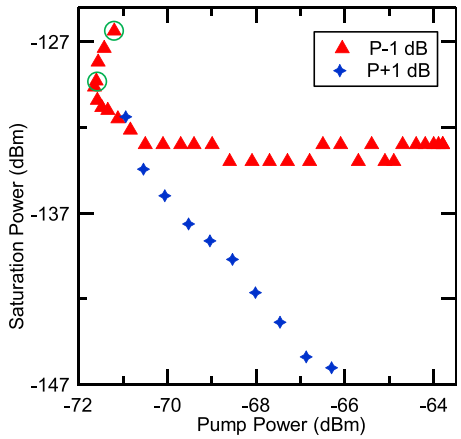

FIG. 4. $P_{\pm 1\mathrm{dB}}$ point for different pump powers. The $P_{-1\mathrm{dB}}$ data show the saturation of the dynamic range on the positive detuning side, while the $P_{+1\mathrm{dB}}$ data show that the dynamic range keeps decreasing as the pump power increases. Green circles indicate the two optimal points.

previously published data (for example in Ref. 16). The discrepancy between the measured saturation power and the calculated values is mainly due to uncertainty in the energy participation ratios which determine the Kerr coefficients used in the calculation [Eqs. (S4), (S14), and (S15) in the supplementary material].

Gain saturation is summarized in Fig. 4, colored by which limit (± 1 dB) is reached first. For positive detuning, the $P_{-1\mathrm{dB}}$ (red triangles) limit is relevant and falls to a static value even as P_p continues to climb for increased detuning. For negative detuning, the $P_{+1\mathrm{dB}}$ (blue diamonds) behavior is limiting and falls steadily with increasing P_p as the amplifier's response becomes increasingly distorted. The two optimum points are circled, and both are near the lowest pump powers, in direct contradiction to the expectations of pump depletion theory that bias conditions requiring stronger pump should yield higher saturation powers.

We note that although this result suggests that the JPC possesses only one best bias point for each bias flux, by jointly varying the pump frequency and flux, the device should be no less tunable. In fact, our result suggests that the device can be readily tuned by jointly varying flux and pump frequency to minimize the pump power required for a given signal frequency. Finally, we add a caution that this picture can be severely disrupted by variation in the impedance presented by the microwave lines connected to the device modes, unless great care is taken to minimize reflections and mismatches in the microwave cabling. In our experiment, this is the dominant source of disagreement between theory and experiment, as the device bandwidth is observed to vary significantly for the range of frequencies at which we recorded gain data. However, at all bias points, the overall behavior of Kerr-based shifts to lower frequencies dominated the device performance and allowed us to identify optimal bias conditions.

In conclusion, we have developed a theoretical treatment which neglects the dynamics and depletion of the microwave pump and focuses on the fourth-order Kerr terms as the source of amplifier saturation. Our data and calculations are in excellent qualitative agreement, and we identify an efficient paradigm for operating three-wave parametric amplifiers in the presence of Kerr nonlinearity. Our results also have vital implications for recent efforts to build multi-parametric Josephson devices, such as directional amplifiers and circulators.[21,27–29] These devices require the delicate matching of several parametric processes spanning multiple modes, providing a very difficult challenge to tune up if the modes themselves move with changing pump conditions. The fourth-order theory can be readily extended to these devices and will provide much needed insight into both bias conditions and saturation behavior.

However, to make substantial improvements in device performance, we must eliminate unwanted higher-order terms through Hamiltonian design. We calculate that a reduction in Kerr term amplitude translates to an equal increase in saturation power until either pump depletion or the sixth-order terms dominate the device response. There has been a very recent effort to achieve such a reduction by using an asymmetric flux-biased Josephson circuit (the so-called "SNAIL") to replace the individual junctions in the JRM.[30]

See supplementary material for the details of the JPC dynamics with only 3rd order couplings and with both 3rd and 4th order couplings.

The authors wish to acknowledge work by E. Brindock and A. Rowden on control software. This manuscript is based upon work supported in part by the U.S. Army Research Office under Grant No. W911NF-15-1-0397.

[1]R. Vijay, D. H. Slichter, and I. Siddiqi, Phys. Rev. Lett. **106**, 110502 (2011).
[2]M. Hatridge, S. Shankar, M. Mirrahimi, F. Schackert, K. Geerlings, T. Brecht, K. M. Sliwa, B. Abdo, L. Frunzio, S. M. Girvin, R. J. Schoelkopf, and M. H. Devoret, Science **339**, 178 (2013).
[3]J. D. Teufel, T. Donner, D. Li, J. W. Harlow, M. S. Allman, K. Cicak, A. J. Sirois, J. D. Whittaker, K. W. Lehnert, and R. W. Simmonds, Nature **475**, 359 (2011).
[4]C. Eichler, D. Bozyigit, and A. Wallraff, Phys. Rev. A **86**, 032106 (2012).
[5]T. Yamamoto, K. Inomata, M. Watanabe, K. Matsuba, T. Miyazaki, W. D. Oliver, Y. Nakamura, and J. S. Tsai, Appl. Phys. Lett. **93**, 042510 (2008).
[6]R. Vijay, M. H. Devoret, and I. Siddiqi, Rev. Sci. Instrum. **80**, 111101 (2009).
[7]A. Roy and M. H. Devoret, C. R. Phys. **17**, 740 (2016).
[8]B. Yurke, L. Corruccini, P. Kaminsky, L. Rupp, A. Smith, A. Silver, R. Simon, and E. Whittaker, Phys. Rev. A **39**, 2519 (1989).
[9]M. Castellanos-Beltran, K. Irwin, G. Hilton, L. Vale, and K. Lehnert, Nat. Phys. **4**, 929 (2008).
[10]M. Castellanos-Beltran and K. Lehnert, Appl. Phys. Lett. **91**, 083509 (2007).
[11]M. Hatridge, R. Vijay, D. H. Slichter, J. Clarke, and I. Siddiqi, Phys. Rev. B **83**, 134501 (2011).
[12]J. Mutus, T. White, E. Jeffrey, D. Sank, R. Barends, J. Bochmann, Y. Chen, Z. Chen, B. Chiaro, A. Dunsworth, J. Kelly, A. Megrant, C. Neill, P. J. J. O'Malley, P. Roushan, A. Vainsencher, J. Wenner, I. Siddiqi, R. Vijay, A. N. Cleland, and J. M. Martinis, Appl. Phys. Lett. **103**, 122602 (2013).
[13]C. M. Caves, Phys. Rev. D **26**, 1817 (1982).
[14]J. Y. Mutus, T. C. White, R. Barends, Y. Chen, Z. Chen, B. Chiaro, A. Dunsworth, E. Jeffrey, J. Kelly, A. Megrant, C. Neill, P. J. J. O'Malley, P. Roushan, D. Sank, A. Vainsencher, J. Wenner, K. M. Sundqvist, A. N. Cleland, and J. M. Martinis, Appl. Phys. Lett. **104**, 263513 (2014).
[15]T. Roy, S. Kundu, M. Chand, A. M. Vadiraj, A. Ranadive, N. Nehra, M. P. Patankar, J. Aumentado, A. A. Clerk, and R. Vijay, Appl. Phys. Lett. **107**, 262601 (2016).
[16]B. Abdo, A. Kamal, and M. Devoret, Phys. Rev. B **87**, 014508 (2013).

[17]F. D. O. Schackert, "A practical quantum-limited parametric amplifier based on the Josephson ring modulator," Ph.D. thesis (Yale University, 2013).
[18]C. Eichler and A. Wallraff, EPJ Quantum Technol. **1**, 2 (2014).
[19]N. Bergeal, R. Vijay, V. E. Manucharyan, I. Siddiqi, R. J. Schoelkopf, S. M. Girvin, and M. H. Devoret, Nat. Phys. **6**, 296 (2010).
[20]N. Bergeal, F. Schackert, M. Metcalfe, R. Vijay, V. E. Manucharyan, L. Frunzio, D. E. Prober, R. J. Schoelkopf, S. M. Girvin, and M. H. Devoret, Nature **465**, 64 (2010).
[21]F. Lecocq, L. Ranzana, G. A. Peterson, K. Cicak, R. W. Simmonds, J. D. Teufel, and J. Aumentado, Phys. Rev. Appl. **7**, 024028 (2017).
[22]B. A. Kochetov and A. Fedorov, Phys. Rev. B **92**, 224304 (2015).
[23]N. Roch, E. Flurin, F. Nguyen, P. Morfin, P. Campagne-Ibarcq, M. H. Devoret, and B. Huard, Phys. Rev. Lett. **108**, 147701 (2012).
[24]E. Flurin, N. Roch, F. Mallet, M. H. Devoret, and B. Huard, Phys. Rev. Lett. **109**, 183901 (2012).
[25]R. Vijay, "Josephson Bifurcation amplifier: Amplifying quantum signals using a dynamical bifurcation," Ph.D. thesis (Yale University, 2008).
[26]*The Duffing Equation: Nonlinear Oscillators and Their Behavior*, edited by I. Kovacic and M. J. Brennan (Wiley, 2011).
[27]L. Ranzani and J. Aumentado, New J. Phys. **16**, 103027 (2014).
[28]A. Metelmann and A. A. Clerk, Phys. Rev. X **5**, 021025 (2015).
[29]K. M. Sliwa, M. Hatridge, A. Narla, S. Shankar, L. Frunzio, R. J. Schoelkopf, and M. H. Devoret, Phys. Rev. X **5**, 041020 (2015).
[30]N. E. Frattini, U. Vool, S. Shankar, A. Narla, K. M. Sliwa, and M. H. Devoret, Appl. Phys. Lett. **110**, 222603 (2017).